

promoting access to White Rose research papers



Universities of Leeds, Sheffield and York
<http://eprints.whiterose.ac.uk/>

This is the author's post-print version of an article published in the **Journal of Colloid and Interface Science**

White Rose Research Online URL for this paper:

<http://eprints.whiterose.ac.uk/id/eprint/78253>

Published article:

D'Souza-Mathew, M, Cayre, OJ, Hunter, TN and Biggs, SR (2013) *Facile synthesis of gold core-polymer shell responsive particles*. *Journal of Colloid and Interface Science*, 407. 187 - 195. ISSN 0021-9797

<http://dx.doi.org/10.1016/j.jcis.2013.06.046>

Facile synthesis of gold core - polymer shell responsive particles

Mark D'Souza Mathew*, Olivier J. Cayre, Timothy N. Hunter and Simon Biggs

*Institute of Particle Science and Engineering
School of Process, Environmental and Materials Engineering
University of Leeds, Leeds, LS2 9JT*

*Email: sms5mdm@leeds.ac.uk

Abstract

The free adsorption of an end-functionalised weak polybase, poly dimethylaminoethyl methacrylate (pDMAEMA), on the surface of colloidal gold nanoparticles (AuNPs) as a route to produce a responsive core-shell nanoparticle is explored here. Optimal conditions for the physisorption of the polymeric chains onto the colloidal nanoparticles are explored. A dense coverage is facilitated by rapidly mixing the well solvated pH responsive homopolymer, at low pH, into a relatively poor solvent environment, at higher pH, containing a stable dispersion of charge-stabilized gold nanoparticles. The rapid pH change causes the polymer chains to concurrently collapse and adsorb onto the gold nanoparticles. In order to achieve sterically stable, monodisperse and responsive core shell nanoparticles, a crucial factor is the pH difference of the systems prior to their mixing. Once adsorbed, end-functional thiol groups on the adsorbed polymer chains can form more permanent covalent attachments with the core particles. Dynamic light scattering coupled with mobility data of pH titration experiments show that the core-shell particles exhibit a responsive character consistent with the observed potentiometric titration data of the polymer. The same particles demonstrate reversible aggregation when cycled between pH extremes. This is confirmed by shifts in the SPR peak of the corresponding UV-Vis absorption profile. The ease and flexibility of this strategy for core-shell particle production, coupled with the stability and responsiveness of the product, make this a promising colloidal coating mechanism.

1 Introduction

Responsive core-shell nanoparticles have been regularly studied for their potential uses in drug delivery [1-3], emulsification and interfacial stabilisation [4-6], interfacial transport [7, 8] and environmental sensor technologies [9-11]. Their properties can also be manipulated to provide functionality when used as building blocks of larger structures such as microcapsules [12] and membranes [13, 14]. At present, the popular methods [15-38] for the synthesis of responsive solid core-polymer shell hybrid particles are: polymer 'grafting-from' the particle surface; a one pot synthesis where the particles are synthesized in the presence of the polymer that acts as a stabilizer; and, finally, polymer 'grafting-to' pre-synthesized particle cores.

In the 'grafting-from' technique, a dispersion of core nanoparticles is first coated with an initiator group [15-21]. Living polymerization is then carried out from these sites to form a dense end grafted brush like polymeric shell. In addition to the high grafting density, control over core size and the polymeric shell swelling range are known advantages. Limitations include a shell thickness that is difficult to control, long synthesis times and the use of harmful solvents [22].

Alternatively in the one-pot synthesis method [23-27], the core particles are synthesized in the presence of end functionalized polymer chains. Due to the end group affinity for the core particles, these polymer chains function as ligand stabilizers for the growing nanoparticles. Whilst it is possible to manipulate the reaction stoichiometry to gain some control over nucleation and growth, the final core particle size is limited to a few nanometers, and in the case of gold cores exhibits a deviation of about 20% in size distribution [28]. A good density of end grafted polymer and long-term stability of the polymer-stabilized colloids are known advantages.

'Grafting-to' [22, 29-38] is now the accepted nomenclature for post modification of the surface of a colloidal dispersion using pre-synthesized polymers. Boyer et al [29] showed how a chemical affinity could result in the directed adsorption of functional end groups (thiol and trithiocarbonate) of block copolymers constructed from PEG analogues onto the surface of citrate-stabilized gold nanoparticles (AuNPs). The

polymer strands were incubated with the gold particle for just 30 minutes before purification. Other noteworthy examples of such thiol affinity based polymer adsorption onto pre-synthesized gold cores include adsorption of PDMA-SH (Zhou et al [30]) and PPA-SH (Zhu et al [9]). The former reportedly requires an incubation time of 72 hours, while a week long duration is required of the latter. Thiol linkers have also been shown to covalently bind DNA onto gold particles [31, 32]. Grafting-to has also been demonstrated with the introduction of CdS quantum dots to an aqueous solution containing thiolated pNIPAM chains [33]. The reaction time for the same was 72 hours and the resultant particles acquired the thermosensitive character of the polymer shell. A variant of this technique involved immobilizing PEOX and P4VP onto silica nanoparticles using perfluorophenylazide (PFPA) as a link molecule which form anchors with the base nanoparticle, and covalent bonds with the polymer species when irradiated with UV light [34]. This is a two-stage procedure involving functionalization of the silica nanoparticles with PFPA (overnight) followed by polymer attachment (15 minutes UV exposure). A coupling reaction takes up to 2 hours for the grafting of carboxyl end group polymers to the surface of hydroxyl terminated AuNP clusters [35].

Singh and Lyon reported on the surface modification of citrate-stabilized gold cores by the adsorption of NH_2 terminated pNIPAM [36]. Increasing the temperature past the LCST enabled precipitation of the polymeric shell on the core particles. In another example [37], citrate stabilized AuNPs and PS-b-PAA were mixed together in a continuous phase of DMF. The dropwise introduction of H_2O induced a surfactant like assembly of these amphiphilic polymers around the AuNPs, this structure was then permanently fixed by a crosslinking agent. Following the same theme, the coating of citrate-stabilized AuNPs with bovine serum albumin (BSA) through electrostatic interactions has been demonstrated [38]. Non-specific binding has also been shown between single strand DNA and the surface of colloidal gold particles [31, 32].

In this paper, we investigate the conditions necessary to facilitate the rapid adsorption of a pH responsive homopolymer onto a suspension of charged-stabilised gold nanoparticles. In our studies we use a pH responsive [39] end-functionalized homopolymer (pDMAEMA-SH). The citrate stabilized gold nanoparticles (AuNPs)

are synthesized by a nucleation-growth mechanism as proposed by Turkevich [40] and later modified by Frens [41]. Through light scattering characterisation we demonstrate conditions under which a successful adsorption of the polymer onto the surface of the AuNPs can be achieved within minutes. A key aim of this work is that the responsive nature of the polymer is retained in the final character of the core-shell particles. This is investigated through particle size measurements and the aggregation behaviour of the system as the pH is altered.

From the previously mentioned classifications of core-shell particle synthesis, this method has similarities with a grafting-to approach. The incubation times before purification of excess polymer are relatively low, and limited only by the rate of polymer deprotonation. In addition, the entire experiment is conducted in an aqueous environment with minimum organic solvent waste, thus enhancing its green chemistry credentials. The broad applicability of this approach should enable triggered surface modification of a variety of colloidal systems for the purpose of stability control or for the synthesis of composite particles.

2 Materials and Methods

2.1 Materials

Colloidal dispersions of gold nanoparticles were synthesized using a modified Turkevich method as described by Frens [41]. All glass reaction vessels and storage containers were cleaned with Aqua Regia. The glassware was then rinsed thoroughly with water, followed by scrubbing with Decon surfactant, an acetone rinse, rinsing with copious amounts of DI water and finally ethanol. The glassware was then dried in an oven for a minimum of 30 minutes. 100 ml of a 0.25 mM HAuCl_4 aqueous solution was stirred with a magnetic bead in a 250 ml round bottom flask immersed in an oil bath that was maintained at 100 °C. The system was given a minimum of 15 minutes to achieve thermal equilibrium. At that point, 1ml of ~ 35 mM $\text{Na}_3\text{Citrate}$ was introduced into the vortex caused by the stirring, and the reaction was allowed to proceed for 30 minutes at the elevated temperature. The flask was then removed from the oil bath and immediately immersed into an ice bath to neutralize the effect of the citrate. After purification through a disposable 0.2 μm cellulose acetate membrane

filter, each stock gold nanoparticle solution was stored in a refrigerator in an opaque container.

The gold nanoparticles were initially sized by light scattering using a Malvern Zetasizer ZS (Malvern Instruments, UK). They were subsequently further analysed using TEM. The dimensions of several hundred particles from these Transmission Electron Micrographs were identified and analysed using CellProfilerTM software [42]. Data from the TEM analyses were found to be in good agreement with the size distributions measured using light scattering (See supporting information).

The polymer used in this study was synthesized using Reversible Addition Fragmented chain Transfer (RAFT) polymerisation. Monomers of DMAEMA were combined with 4-Cyanopentanoic acid dithiobenzoate, 4,4-Azobis(4-cyanopentanoic acid) and dioxane in an ampule followed by purging in nitrogen. Reaction was initiated by heating in an oil bath (at 70°C) and terminated after 12h by cooling in an ice bath. Purification was performed by multiple heptane precipitations. The dithioester moiety was reduced to a thiol group using Sodium Borohydride (NaBH₄) followed by vacuum drying overnight. The chain length was verified by NMR and found to be 129 units; giving a molecular weight of 20313 g mol⁻¹ and a rigid rod length of approximately 20 nm.

2.2 Methods

2.2.1 The adsorption process

The dried and purified polymer was dissolved in water at pH 2 to give an aqueous solution at a concentration of 7.2 wt%. The initially low pH facilitates protonation of the tertiary amines and hence solvation of the polymer chains. Over 72 hours of continuous stirring, the pH slowly increased to 6.8 due to the proton consumption by the amine groups. The polymeric dispersion was then divided into two aliquots; one was reduced to pH 3.8 and the other to pH 6. Test tubes containing 12 ml of the stock gold nanoparticle solution were adjusted to pH's 7, 10 and 11, and then magnetically stirred. Aliquots of the aforementioned pH adjusted polymer solutions were introduced into the stirring vortex, and the samples were then left stirring for 30 minutes at room temperature. The polymer concentration was calculated to be in

excess (~50x) of that needed for full surface coverage assuming rapid physisorption to the available gold surface area (calculated using the radius of gyration (R_g) for the polymer and assuming no relaxation of the polymer at the surface).

Next, 1 ml of the as-prepared sample was introduced to a set of 12 Eppendorf 1.5 ml centrifuge vials containing 0.5 ml of pH 3 Milli-Q water. The vials were gently agitated before centrifuging at 14,500 rpm for 30 minutes. 1.4 ml of supernatant was removed and replaced with fresh pH 3 Milli-Q water. This procedure was repeated 3 times to remove excess unbound polymer. It is noted that due to the possibility of damaging or gelling the particles with repeated centrifugation, great care had to be taken in the wash cycles to not over compress the consolidated beds.

2.2.2 Hydrodynamic diameter and mobility study

The hydrodynamic diameter of the particles across a range of pH from 2 to 11 was measured using dynamic light scattering (Malvern Zetasizer[®], Malvern Instruments, UK). The same instrument was used to determine the electrophoretic mobility of the particles across the same pH range. All light scattering experiments were conducted using disposable cuvettes in chambers equilibrated to 20 °C.

The samples were also studied using a UV-Vis Spectrophotometer. Samples were prepared in cleaned (in Decon, water, ethanol and then dried) 1 cm path length cuvettes, placed in the temperature controlled measurement chamber of an Agilent UV Vis Spectrophotometer 8453 after calibrating the instrument with cuvette containing MilliQ water. Measurements were taken across the spectrum at a temperature of 20°C. Particular attention was paid to the location and shape of the Surface Plasmon Resonance (SPR) peak, which is expected to be located at 520 nm for the ratio of reactants used in this synthesis [43]. In order to illustrate differences in peak shift and profile broadening, the UV-Vis profiles of grafted-to core-shell nanoparticles were normalized to the absorbance units of the core AuNPs.

For the titration experiments, a sample of stable core-shell particles was subjected to centrifugation/re-dispersion cycles in pH 7 Milli-Q water before being divided into two equal volumes. By sequential addition of microlitre quantities of 1M HNO₃ or

KOH, each half was adjusted towards acidic and basic extremes. Hydrodynamic diameter and mobility data were recorded at specific intervals.

2.2.3 Electron microscopy

Transmission Electron Microscopy (TEM) images were obtained from a Philips CM200 Field Emission Gun TEM operating at 200 kV. The hybrid particles were imaged on a holey carbon TEM grid. For particles positioned on the carbon film, it was not possible to resolve the polymeric halo due to blending with the carbon substrate. Particles positioned with edges hanging over holes provided the best resolution of the polymeric shell (See supporting info). However in practice, the halo thus characterised around each particle began to show signs of broadening over 300 seconds due to the electron beam. To minimize the occurrence of these beam damage artefacts, images were obtained within 5 seconds of centering on the required particles.

2.2.4 Potentiometric titration of the unbound polymer

The charging behaviour of the polymer was characterised using a potentiometric titration from an acidic to basic direction. 0.1005g of dried pDMAEMA₁₂₉-SH was dissolved in 20 ml of pH 2 Milli-Q water. After stirring for four days, the pH was measured and readjusted with a small amount of HNO₃ and measured the following day at pH 1.73. 100µl of 10mM KOH was added and the stable pH value was noted. This step was repeated multiple times until the final measured pH reached a value of 11. Variations in pH for total volume of base were noted and plotted accordingly. The same data was used to plot the trend in degree of protonation as a function of pH, as shown in Figure 1.

2.2.5 pH cycling

To demonstrate reversible aggregation, the most stable particle suspension (as ascertained by light scattering and spectroscopic analysis, see section 3.2) was centrifuged using the aforementioned parameters. The supernatant was then replaced by either pH 3 or pH 11 Milli-Q water. After this, the vials were subjected to a 5 minute agitation in an ultrasonic bath, followed by 2 minutes in a vortex mixer. The above procedure was repeated three times for each point to ensure that the particles

were indeed dispersed at the required pH. The particle size distribution (measured through light scattering) was measured and evidence of aggregation further studied using the UV-Vis Spectrophotometer, in a similar procedure to that outlined in section 2.3, at each pH for three complete cycles.

3 Results and Discussion

3.1 Expected adsorption from degree of polymer protonation

The main adsorption mechanism behind this variant of the ‘grafting-to’ strategy relies on manipulation of the solvency of the medium for the shell polymer (pDMAEMA-SH), which varies with pH. Rapid adsorption is enabled here by triggering a sudden conformational change of the polymer in the presence of colloidal particles. In a good solvent, the polymer adopts an extended conformation. When introduced to a poor solvent, a change of conformation is expected wherein the polymer chains collapse to a compact (coil) conformation. This may also lead to flocculation or phase separation of the polymer. However, in the presence of a solid interface such as a colloidal dispersion, the polymers may instead preferentially adsorb onto the available solid surface.

The mixing of a polymer solution with a suspension of nanoparticles may in any case, and regardless of changes in solvency, lead to unwanted effects such as bridging flocculation. Consequently, in order to maintain colloidal stability throughout the procedure described here, one needs to introduce a sufficient amount of polymer to saturate the available colloidal surface area. In the system discussed here, the surface of the gold colloid is negatively charged at all pH values tested and the polymer chosen for the reaction is positively charged at low pH, in which case a strong adsorption is expected due to these electrostatic interactions. At basic pH values the polymer is neutral and water becomes a poor solvent, which is also expected to drive strong adsorption onto the colloid surface. The relative adsorbed amounts will however be very different at these different pH conditions with adsorption density being maximised in the poor solvent conditions.

In the experimental protocol described here, we take a polymer dissolved in good solvent conditions and mix it with a colloidal dispersion such that the mixing results in a rapid pH change to a poor solvent environment. We expect then that the introduction of an appropriate concentration of well solvated ‘extended’ polymer into a poor solvent will result in two simultaneous effects: a rapid change to a more ‘compact’ conformation for the polymer, and a subsequent adsorption at the solid-liquid interface.

Potentiometric titration data (See supporting information) show that the rate of change of pH with respect to base addition ($dpH/dMEB$) indicates the onset of deprotonation (large peak) at pH 4.5 and complete deprotonation at pH 9.1 (small peak). The data in Figure 1 represents the derived degree of protonation as a function of pH. At all pH < 4, the polymer is fully protonated and it is 50% protonated at pH 6.8. These values will be referred to in later paragraphs to understand how charge density (and hence polymer conformation) influences the interaction with the colloidal dispersion. In the experiments described in this work, mixing of the polymer with a gold colloid suspension at a significantly higher pH will cause some deprotonation of the amine groups along the polymer chain length. Such conditions are expected to drive a rapid polymer adsorption onto the colloidal gold surface. This article explores the pH conditions for both the polymer solution and the gold colloid suspension to achieve this rapid adsorption, while leading to stable polymer-coated gold nanoparticles.

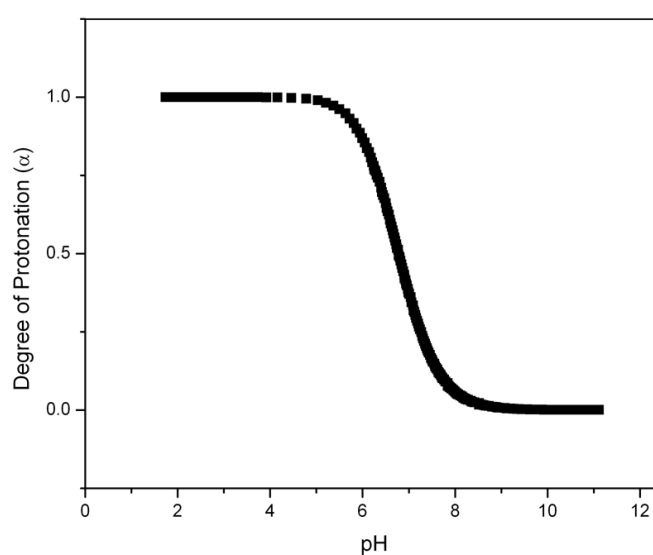


Figure 1: Degree of protonation as a function of pH derived from potentiometric titration of pDMAEMA₁₂₉-SH from pH 1.73 to pH 11.11 (See supporting information)

3.2 Influence of colloidal gold suspension pH

Depending on the pH and extent of polymer deprotonation when introducing the polymer to the AuNP dispersion, a number of mechanisms can cause the particles to aggregate or flocculate. Instability in this binary system may occur through polymeric bridging flocculation, where a single polymeric strand in an open conformation bridges with polymer segments on adjacent nanoparticles. Secondly, an excess of background electrolyte may also compress the stabilizing electric double layer surrounding colloidal particles, reducing the Debye length and thus allowing Van der Waals forces to initiate particle aggregation as the particles approach each other at closer separation distances. Additionally, if a large pH increase causes the grafted polymers to attain an uncharged and tightly bound conformation on the gold surface, the core-shell particles may become hydrophobic and aggregate to reduce the free energy state.

To explore the conditions necessary for an effective and stable coating procedure, the pH values of the binary systems (AuNPs and pDMAEMA) were varied prior to mixing. In each case, dynamic light scattering was used to probe the hydrodynamic diameter of the final particle suspension after completion of the adsorption procedure and removal of the excess polymer. In addition, the UV-vis absorption spectra of each of the samples were recorded and are presented here to complement the size data. The combination of both these measurements allows us to draw conclusions with respect to the structure and the stability of the final suspension of hybrid nanoparticles.

We first present a table showing the initial pH values of both the polymer solution and the gold nanoparticle suspension in addition to the resultant pH values of their mixtures. These are complemented with noticeable changes in stability of the AuNPs where an observed blue shift or precipitation is assumed to be an indicator of colloidal aggregation. Here, well solvated aliquots of polymer at pH 4 (~100% protonation) and pH 6 (~80% protonation) are introduced to AuNPs at pH 7, 10 and 11, where the particles are observed to be colloidally stable.

Pre mixing pH	AuNP pH 7.3	AuNP pH 10	AuNP pH 11
3.8	5.8 (<i>HA</i>)	6.2 (<i>ST</i>)	7.4 (<i>SA</i>)
6	6.2 (<i>SA/ST</i>)	6.6 (<i>ST</i>)	7.6 (<i>HA</i>)

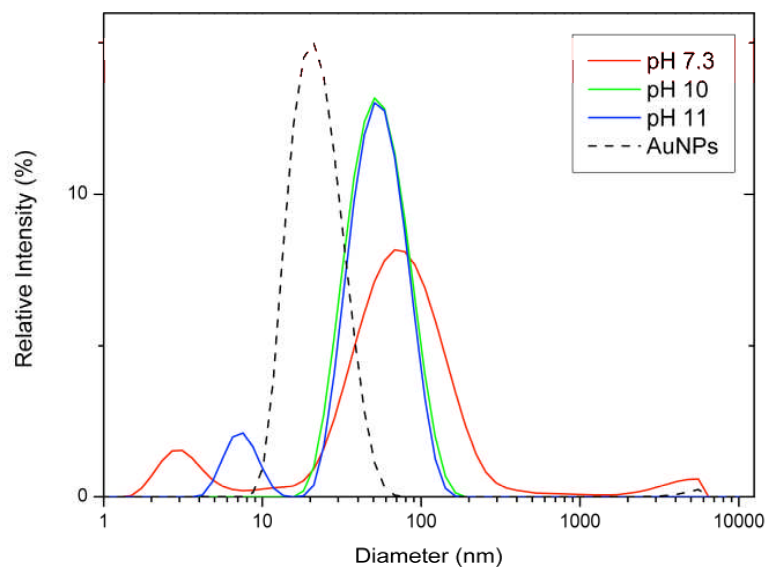
Table 1: Final measured pH values and visual stability examination (*italic*) of the resultant dispersions measured 5 minutes after mixing of the polymer solution and gold nanoparticle suspension at varying pH. Note: *SA* indicates slight-aggregation observed, *HA* indicates heavy-aggregation and *ST* indicates visually stable.

Table 1 shows that under certain pH conditions (i.e. the two extreme conditions of gold nanoparticle suspension pH reported) this procedure yields a system where rapid adsorption of the polymer leads to uncontrolled and irreversible aggregation. Where an intermediate pH was used for the suspension, it appears that the system is stable after mixing. These initial assessments of stability were conducted on the basis of visual observation of the dispersion colour, where simply a shift from bright red to burgundy and indigo was taken as an indication of particle aggregation. These changes were quantified using light scattering and UV-Vis analysis, as described in the proceeding sections.

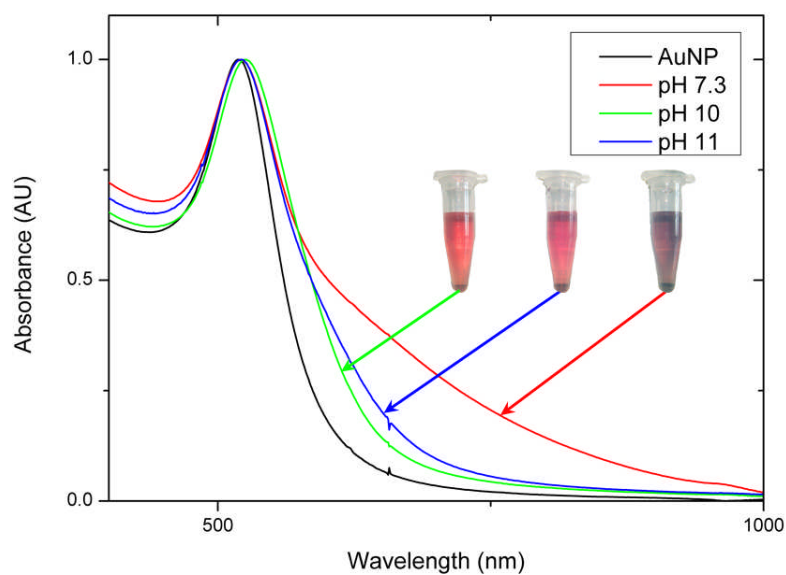
3.2.1 Cases where initial polymer solution pH = 3.8

Figure 2 shows light scattering size measurements (A) and UV-Vis analysis (B) corresponding to experiments where pDMAEMA₁₂₉-SH at pH 3.8 is introduced to 20 nm citrate-stabilised AuNPs at pH 7.3, 10 and 11, respectively. At the initial solution pH of 3.8, the polymer chains are fully protonated (Figure 1) and will therefore adopt an extended conformation in solution. In these three experiments, we test the influence of *in situ* deprotonation and change of conformation for the polymer as it mixes with and adsorbs onto an oppositely charged gold colloid at a different pH. The measurements shown here are made after the mixed sample was washed several times by centrifugation/re-dispersion to remove the excess polymer and the particles were finally re-dispersed in pH 3 water. From Figure 2, all samples show an increase in the measured hydrodynamic diameter and a broadening of the UV-Vis spectra. However, this behaviour is more pronounced in the case where the particles are initially dispersed at the lower pH. An increase in diameter is expected from the adsorption of polymer on the surface of the particles, but in some cases the size increases seen here suggest aggregation/flocculation of the system rather than coating. In addition, the size distribution data also show a small but finite peak in the sub 10 nm range, which

is likely due to the presence of weakly bound polymer in the system: As the prepared hybrid particles are thoroughly washed prior to observation, we believe this peak is the result of longer-term polymer leaching from the surface and can potentially give an indication of the anchoring efficiency.



(A)



(B)

Figure 2: Light scattering data of samples prepared following the procedure described above. The hybrid particles are suspended in pH 3 water for these measurements. Here, the initial pH of pDMAEMA₁₂₉-SH is 3.8 when introduced to citrate stabilized gold nanoparticles at pH 7.3 (red), 10 (green) and 11(blue) (A) Relative Intensity profiles from light scattering measurements (B) UV Vis profiles normalized to the peak intensity of base AuNP profile.

We note that broadening of the UV-Vis spectra is characteristic of instability in gold nanoparticle dispersions. In the case where the initial AuNP pH is 7.3, the UV-Vis profile (Figure 2B) shows significant broadening between 600 and 1000 nm. This suggests a large degree of aggregation in the system, which is confirmed by visual observation of the sample where the indigo colour is indicative of this aggregation. The size distribution data support these observations. It is likely that, in this case, the polymers introduced to the gold nanoparticle suspension are still well solvated and when the system reaches its equilibrium pH, the polymer retains significant protonation (~90% as estimated from Figure 1B). Since the polymer is positively charged, and the particles have an opposite negative surface charge due to the adsorbed citrate ions, it is likely that the polymer will adsorb onto the particle surface through an electrostatic interaction. However, because of its retained extended conformation due to the high charge, there is an increased probability of polymeric bridging between particles. Thus, the apparent aggregation in the system is likely due to bridging flocculation caused by extended polymers forming multiple contacts between adjacent AuNPs.

The UV-Vis profiles for the AuNPs with initial pH values of 10 and 11 show only a small broadening of the spectrum as compared to the base uncoated AuNPs and can be regarded as quite similar. The subtle differences arise on a visual examination, where the sample at initial AuNP pH 10 retains the red colour (Figure 2B insert) of the uncoated nanoparticles, whereas in the case at pH 11, a slight purple hue is observed, which is indicative of a small amount of aggregation in the system. Size distribution profiles (Figure 2A) show a unimodal peak at 50 nm for AuNP pH 10, and a bimodal distribution at AuNP pH 11 with a coinciding 50 nm peak and sub 10 nm component. By consulting the results from Table 1 and Figure 1, at the equilibrium pHs of the mixtures, the polymer retains approximately 80% and 20% protonation when the initial gold nanoparticle suspension is at pH 10 and 11, respectively. Such values are subject to potentially significant errors due to the difficulty in accurately measuring pH around 7 and the fact that the degree of protonation around the pKa (~6.5) also changes very rapidly. What is certain is that the case where the gold nanoparticles are initially at pH 11 will lead to the polymer in the mixture being more deprotonated. It is likely to strongly adsorb onto the particles in a more compact conformation, as water is a poor solvent under these conditions.

Therefore, this is likely to provide a relatively less efficient steric stabilisation of the system and potentially promote poor solvent driven aggregation if the polymer layers grafted on the surface of approaching particles are allowed to come into contact [44].

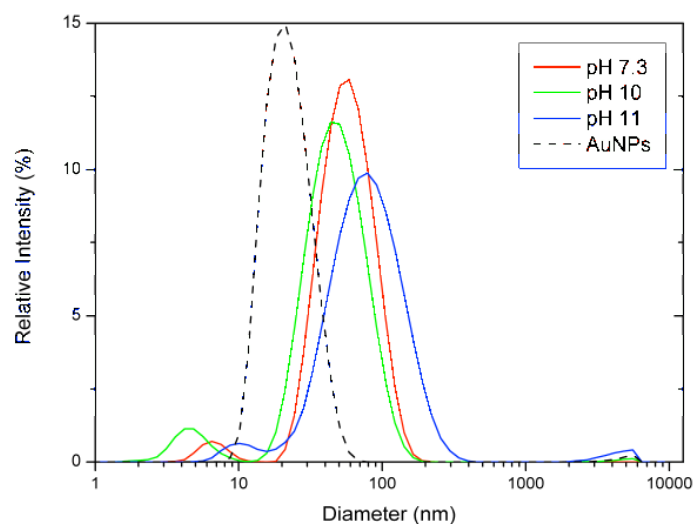
In the case of the reactions carried out with the gold nanoparticle suspension initially at pH 10, the somewhat less basic initial conditions (compared to the pH 11 case) lead to a higher degree of residual polymer protonation at the correspondingly lower equilibrium pH of the mixture. In these conditions, results from Figure 2 suggest the adsorption of the polymer onto the surface leads to hybrid core-shell particles that are stable. Indeed, particle size measurements reveal a monomodal distribution suggesting that no polymer is desorbing from the particle surfaces during the washing steps, or subsequently. Visual observation of the sample suggests no aggregation and the UV-Vis spectrum shows only a small variation as compared to that of the initial gold nanoparticle suspension. This stability is further verified by examination of the TEM micrographs (See supporting information) showing that the coated particles are indeed distinct, and have resisted significant clustering from capillary action during drying. In these particular conditions, one can deduce that the polymer adsorption is efficient and that the configuration and degree of protonation of the polymer on the particle surface is suitable for efficient steric stabilisation and to avoid significant desorption.

3.2.2 Cases where initial polymer solution pH = 6

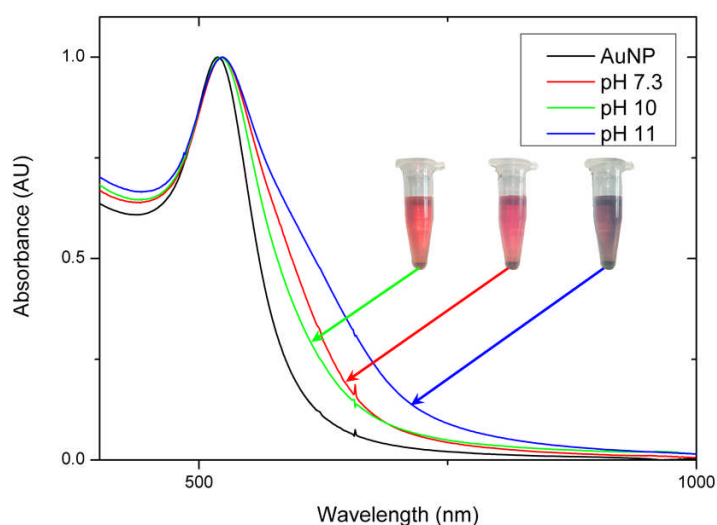
Next, we consider the profiles from Figure 3, showing size measurements (A) and UV-Vis analysis (B) where the initial pH of the polymer is kept constant at 6. In this case, during the adsorption procedure, the initial polymer conformation is expected to be less extended when compared to pH 3.8, as a result of the reduced polymer charge. Again, the data presented in this section (Figure 3) was obtained for coated samples that have been washed 3 times and re-dispersed at pH 3.

In the first case where the gold nanoparticle suspension is initially at pH 7.3, the UV-Vis spectrum (Figure 3B) shows slight broadening, a visual observation reveals a slight change in colour of the final dispersion and the size distribution data shows a bimodal distribution. In comparison to the previous case, the polymer after mixing is

likely to be less protonated and will thus adopt a less extended configuration. This will reduce the magnitude of bridging flocculation. The slight colour change and UV-Vis spectrum, where the peak broadening appears much less significant are in agreement with this hypothesis. However, the bimodal distribution of the size data again suggests that there still is some desorption of the polymer.



(A)



(B)

Figure 3: Light scattering data of samples at pH 3. Here, the initial pH of pDMAEMA₁₂₉-SH is 6 when introduced to citrate stabilized gold nanoparticles at pH 7.3 (red), 10 (green) and 11 (blue) (A) Relative Intensity profiles from light scattering measurements (B) UV-Vis profiles normalized to the peak intensity of base AuNP profile.

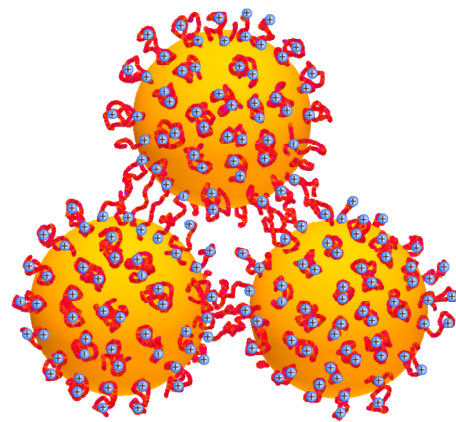
The UV-Vis profile of the hybrid system for an initial nanoparticle suspension at pH 10 shows, as seen previously, the least deviation from the initial AuNPs suspension spectrum and the sample retains the same vibrant red colour (shown in Figure 3B). In

this case, however, the size distribution data shows a bimodal sample suggesting some desorption of polymer from the particle surface unlike the example at pH 3.8. However, the measured hydrodynamic diameter (~45 nm) of the polymer-grafted particles in this case also appears to be in agreement with the presence of a dense polymer layer (20 nm core + 10-12 nm polymer layer thickness) on the particle surface, suggesting that any polymer desorption is minimal. As discussed above for the unbound pre-synthesised polymer (section 2.1), an end grafted and fully extended chain of pDMAEMA₁₂₉ would contribute approximately 20 nm to the measured hydrodynamic diameter. Hence, the 12.5 nm contribution is quite reasonable for a layer of adsorbed polymer in a semi-collapsed conformation. One can conclude from these observations that hybrid systems obtained by precipitating the polymer onto the surface of the gold nanoparticle suspensions at pH 10 were stable, for samples at both initial pH conditions of the polymer solution. In both cases the resulting polymer layer appears suitable for efficient steric stabilisation of the system during the adsorption procedure.

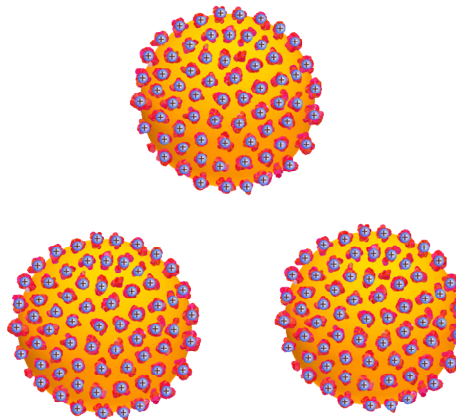
A distinct shoulder indicating the presence of aggregates is observed in the UV-Vis spectrum (Figure 3) when the gold nanoparticle suspension is used at pH 11. This is much more pronounced than for the same dispersion with an initial polymer solution pH of 3.8 (shown in Figure 2). Similarly, the size distribution data also show a peak occurring at larger diameters (as compared with the case where the initial polymer solution pH is 3.8). Additionally, this sample showed significant colour change. In this case, the relatively low protonation of the polymer prior to mixing is likely to drive a fast adsorption of the polymer on the available surface. In addition the conformation of the polymer on these gold nanoparticles is likely to be compact as water becomes a poor solvent for the polymer in these conditions. Again, this will drive aggregation due to the poor solvency effects in the composite system. Additionally, the greater amount of electrolyte added to increase the initial polymer pH may also enhance coagulation due to the reduction in Debye length at this pH, which is possibly why the system appears more aggregated than for systems where the polymer is initially at pH 3.8.

To summarise the likely behaviour of the system in all cases experimentally explored above, we have represented the three likely phenomena responsible for the different

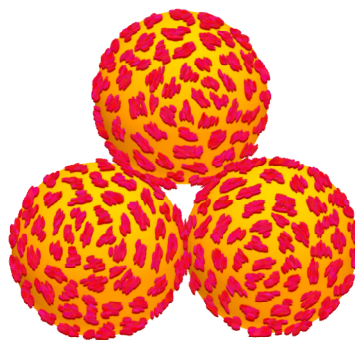
behaviours, viz. bridging flocculation, steric stabilisation and intersegment attraction forces, in a schematic given in Figure 4.



(A)



(B)



(C)

Figure 4: Schematics showing degrees of the three expected behaviours of pDMAEMA adsorbed on a AuNP dispersion as a function of the charge on the polymer. The initial AuNP dispersion pH value is (A) 7.3 *highly charged polymer chains* (B) 10 *partially charged polymer chains* (C) 11 *uncharged chains*.

For well solvated polymers, introduced to a good solvent containing stable AuNPs, as in the cases when the pH of the colloidal dispersion is 7.3, varying degrees of aggregation have been observed, which is attributed to bridging flocculation (schematically shown in Figure 4A).

Figure 4B describes the instances when the colloidal dispersion is at pH 10 and illustrates the efficient adsorption of polymers that are partially deprotonated as a result of their environment pH onto the AuNP surface. The residual charge on the polymer in this pH range creates a steric layer sufficient to provide stability of the hybrid system as demonstrated in our experiments.

In our experiments, when the polymer is introduced to a colloidal dispersion at pH 11, and with knowledge of the equilibrium pH of the mixture, the polymer layers become almost totally deprotonated. The resultant low solubility drives the polymers to adsorb strongly onto the colloidal surface. The low degree of charge on the adsorbed polymer and its low affinity for the water solvent is likely to lead to a compact layer and subsequent aggregation caused by attractive intersegment forces [44] for polymer coated surfaces coming together in a poor solvent (Figure 4C).

3.3 Titration study: Size & mobility

In order to demonstrate a successful adsorption of the polymer on the surface of the gold nanoparticles further, we examine the pH-responsive behaviour of the stable hybrid system produced when initial pHs of pDMAEMA and AuNPs are 6 and 10, respectively. Initially, we perform an isotherm titration of particle hydrodynamic diameter and electrophoretic mobility as a function of pH. This is presented in Figure 5, where we observe mobility data that seem in line with the measurements of the degree of polymerisation of the polymer presented in Figure 1B. In particular, the complete loss of mobility around pH 8 seen in Figure 5 is substantiated by a zero degree of protonation at the same pH for the bare polymer. In the hybrid system, the contraction of the polymer on the surface of the gold nanoparticles, due to its low solubility at this pH, seems to induce some aggregation in the system. This is confirmed by both the hydrodynamic diameter measurements and UV-Vis measurements presented in the subsequent graphs. On the other hand, as the polymer on the surface of the particles protonates (between pH 6 and 8), the hydrodynamic

diameter recorded decreases (when moving from basic pHs). This indicates that as expected, upon protonation and extension of the polymer away from the particle surface, the particles become stable and no aggregation is observed. Additionally, the diameter recorded (between 40-60 nm) is in reasonable agreement with calculations for an extended polymer layer on the surface of a gold nanoparticle core of 20 nm. These results also correlate well to some of our previous work, on the responsive behaviour of latex particles grafted with polymers of the same type [45].

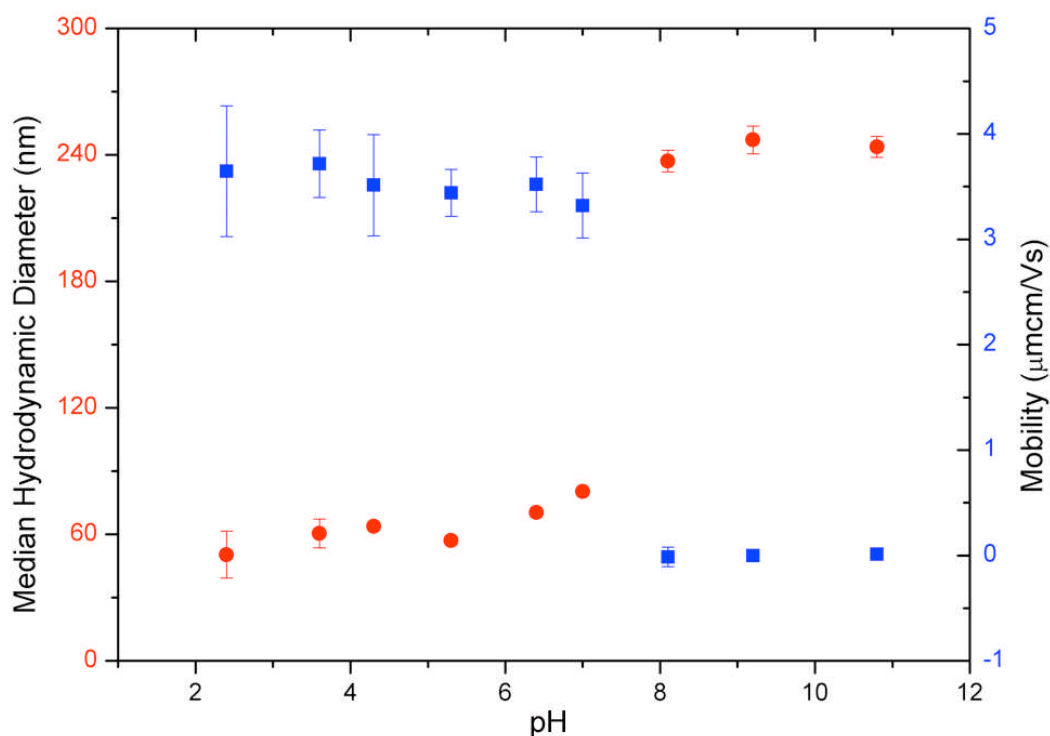


Figure 5: Titration of stable 'grafted-to' particles showing trend in aggregation ascertained by the median hydrodynamic diameter (Red circles) and particle mobility (Blue squares). The ionic strength at both pH extremes is approximately 20 mM.

Therefore, results from the hydrodynamic diameter and mobility study demonstrate that the hybrid particle system prepared retains the pH responsive nature of the adsorbed polymer. Secondly, the response of the polymer shell is responsible for altering the stability of the system as a function of pH and can be used to control the colloid stability of the system. In the next section, we demonstrate how the same responsive component can be manipulated to show reversible aggregation.

3.4 pH cycling

The same stable hybrid particles were used here to investigate the reversibility of the aggregation induced by pH change. To accurately change pH without screening arising from electrolyte build up, centrifugation is used in this case to separate the particles and subsequently replace the continuous phase. Effects such as collapse and swelling of the polymeric layer on individual particles may not be resolved due to particle impaction from the processing technique. Instead, redispersion of aggregates was monitored. In addition to dynamic light scattering measurements, surface plasmon resonance (SPR) shifts of the UV-Vis profiles are good indicators for monitoring reversible aggregation, and the results are given in Figure 6.

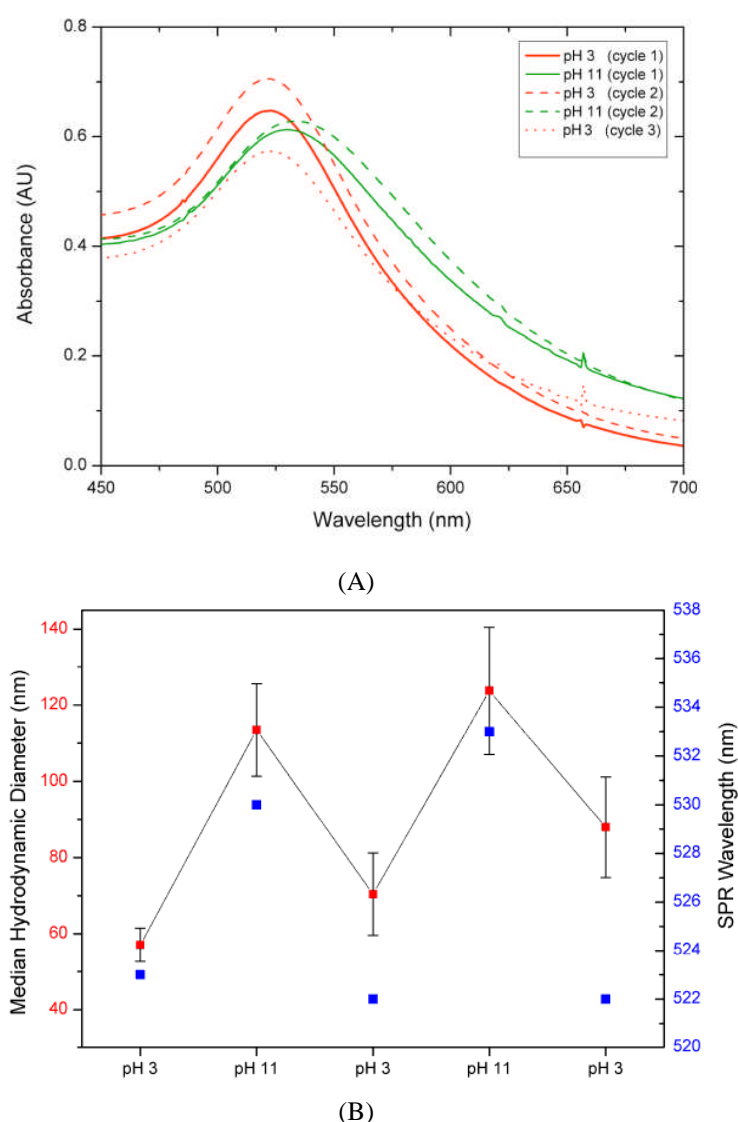


Figure 6: (A) UV-Vis profiles of sterically stable pH responsive particles exhibiting pH cycling between values 3 and 11. (B) Median hydrodynamic diameter values recorded at different pHs during the cycling of a successfully grafted gold particle suspension (red squares) and corresponding variations in SPR from UV-Vis spectroscopy measurements (blue squares)

The UV-Vis profiles of these hybrid particles (Figure 6A) show a 10 nm red shift in SPR as the sample is cycled from pH 3 to pH 11 indicating the presence of aggregates. Additionally when cycled to pH 11, a broadening of the peak shoulder is observed in relation to pH 3. When the pH is changed back to 3, the SPR returns to its initial value suggesting that a majority of the particles have re-dispersed efficiently upon protonation of the polymer layers. This same cycled responsive behaviour was characterised for a further two cycles, however some degree of hysteresis was evident (increased peak broadening at pH 3) suggesting perhaps incomplete re-stabilisation with further cycles. Hydrodynamic diameter values averaged over 20+ runs show a distinct difference for particles re-dispersed at pH 3 and 11, respectively. The data presented in Figure 6B combines the peak median values from light scattering intensity data with the SPR data to show a similar trend to that observed in Figure 6A. Here, after initial aggregation from pH 3 to 11, the reported values do not suggest complete recovery to the original monodisperse and stable state. Instead, there is a small increase in the median particle diameter that is likely due to small particle clusters tethered together by well solvated and extended polymer. This is potentially caused by the procedure used to vary pH in this particular experiment (through centrifugation steps), which can induce closer contact of the particles within the sedimented bed than is expected in the bulk. It is important to remember the differences in pH altering technique while comparing these data to that from the titration experiment (Figure 5). Here, sonication is required to redisperse the impacted particles at the bottom of the centrifuge vial, hence the absence of large aggregates as seen in the former experiment. Generally however, this experiment demonstrates that the overall control over stability of the hybrid system is maintained as the pH is cycled.

The evidence that the particles pH responsive nature is robust enough to be, at least, largely maintained with repeated centrifugation cycles is a significant result. Such responsive particles would be perfect candidates to act as interfacial stabilisers in emulsions and foams for instance, where having the ability to switch stability on and off would be beneficial to many applications, one of the most cited ones being the use of such systems for controlled/triggered delivery of active ingredients [46]. The simplicity of their production using benign conditions is an appealing feature.

Although not tested here, the incorporation of an end-functional group in the polymer should lead to irreversible chemical grafting over time.

4 Conclusions

We have investigated and presented conditions necessary to produce responsive monodisperse core-shell particles by manipulating the solvency and thus promoting adsorption of a pH-responsive polymer on the surface of charge-stabilised gold nanoparticles. This procedure is fast and, under the right conditions, leads to stable hybrid systems where the polymer is efficiently adsorbed on the surface of the particles and acts as a steric stabiliser. We have shown that the adsorbed polymeric layer retains its pH responsive behaviour, which can be used to control the stability/aggregation of the hybrid particle dispersion. Such particles exhibit reversible aggregation as the pH of the medium is cycled between 3 and 11, evidenced by changes in the SPR of the UV Vis spectrum. The ultra-fast reaction times of the solvency controlled polymer adsorption in an aqueous environment, indicates its viability as an industrial processing stage for the synthesis of responsive core-shell building blocks. Additionally, the potential flexibility of this technique in allowing separate control of the size and type of the core inorganic or metallic colloidal particles, along with control over the polymer properties means a large range of stimuli responsive composite particulates may potentially be synthesised.

References:

1. Guo M, Yan Y, Zhang H, Yan H, Cao Y, Liu K, Wan S, Huang J, Yue W. Magnetic and pH-responsive nanocarriers with multilayer core-shell architecture for anticancer drug delivery. *J. Mater. Chem.* 2008;18:5104-5112.
2. Veisheh O, Gunn JW, Zhang M. Design and fabrication of magnetic nanoparticles for targeted drug delivery and imaging. *Advanced Drug Delivery Reviews.* 2010;62(3):284 - 304.
3. Yuan Q, Venkatasubramanian R, Hein S, Misra RDK. A stimulus-responsive magnetic nanoparticle drug carrier: Magnetite encapsulated by chitosan-grafted-copolymer. *Acta Biomaterialia.* 2008;4(4):1024 - 1037.
4. Amalvy JI, Unali G, Li Y, Granger-Bevan S, Armes SP, Binks BP, Rodrigues JA, Whitby CP. Synthesis of Sterically Stabilized Polystyrene Latex Particles Using Cationic Block Copolymers and Macromonomers and Their Application as Stimulus-Responsive Particulate Emulsifiers for Oil-in-Water Emulsions. *Langmuir.* 2004;20(11):4345-4354.
5. Dupin D, Armes SP, Fujii S. Stimulus-Responsive Liquid Marbles. *Journal of the American Chemical Society.* 2009;131(15):5386-5387.
6. Binks BP, Murakami R, Armes SP, Fujii S, Schmid A. pH-Responsive Aqueous Foams Stabilized by Ionizable Latex Particles. *Langmuir.* 2007;23(17):8691-8694.
7. Li D, Zhao B. Temperature-induced transport of thermosensitive hairy hybrid nanoparticles between aqueous and organic phases. *Langmuir* 2007;23(4):.
8. Stubenrauch K, Voets I, Fritz-Popovski G, Trimmel G. pH and ionic strength responsive polyelectrolyte block copolymer micelles prepared by ring opening metathesis polymerization. *Journal of Polymer Science Part A: Polymer Chemistry.* 2009;47(4):.
9. Zhu M, Wang L, Exarhos GJ, Li ADQ. Thermosensitive Gold Nanoparticles. *Journal of the American Chemical Society.* 2004;126(9):2656-2657.
10. Nuopponen M, Tenhu H. Gold Nanoparticles Protected with pH and Temperature-Sensitive Diblock Copolymers. *Langmuir.* 2007;23(10):5352-5357.
11. Shen Y, Kuang M, Shen Z, Nieberle J, Duan H, Frey H. Gold Nanoparticles Coated with a Thermosensitive Hyperbranched Polyelectrolyte: Towards Smart Temperature and pH Nanosensors. *Angewandte Chemie International Edition.* 2008;47(12):.
12. Chen Y, Wang C, Chen J, Liu X, Tong Z. Growth of Lightly Crosslinked PHEMA Brushes and Capsule Formation Using Pickering Emulsion Interface-Initiated ATRP. *Polymer.* 2009:.
13. Schepelina O, Zharov I. Poly(2-(dimethylamino)ethyl methacrylate)-Modified Nanoporous Colloidal Films with pH and Ion Response. *Langmuir.* 2008;24(24):14188-14194.

14. Schepelina O, Zharov I. PNIPAAm-Modified Nanoporous Colloidal Films with Positive and Negative Temperature Gating. *Langmuir*. 2007;23(25):12704-12709.
15. Tsuji S, Kawaguchi H. Temperature-Sensitive Hairy Particles Prepared by Living Radical Graft Polymerization. *Langmuir*. 2004;20(6):2449-2455.
16. Raula J, Shan J, Nuopponen M, Niskanen A, Jiang H, Kauppinen EI, Tenhu H. Synthesis of Gold Nanoparticles Grafted with a Thermoresponsive Polymer by Surface-Induced Reversible-Addition-Fragmentation Chain-Transfer Polymerization. *Langmuir*. 2003;19(8):3499-3504.
17. Radhakrishnan B, Ranjan R, Brittain WJ. Surface initiated polymerizations from silica nanoparticles. *Soft Matter*. 2006;2:386-396.
18. Olivier A, Raquez J, Dubois P, Damman P. Semi-crystalline poly(ϵ -caprolactone) brushes on gold substrate via "grafting from" method: New insights with AFM characterization. *European Polymer Journal*. 2011;47(1):31 - 39.
19. Chevigny C, Gimes D, Bertin D, Jestin J, Boue F. Polystyrene grafting from silica nanoparticles via nitroxide-mediated polymerization (NMP): synthesis and SANS analysis with the contrast variation method. *Soft Matter*. 2009;5:3741-3753.
20. Prucker O, Rhe J. Mechanism of Radical Chain Polymerizations Initiated by Azo Compounds Covalently Bound to the Surface of Spherical Particles. *Macromolecules*. 1998;31(3):602-613.
21. Lattuada M, Hatton TA. Functionalization of Monodisperse Magnetic Nanoparticles. *Langmuir*. 2007;23(4):2158-2168.
22. Cayre OJ, Chagneux N, Biggs S. Stimulus responsive core-shell nanoparticles: synthesis and applications of polymer based aqueous systems. *Soft Matter*. 2011;7:2211-2234.
23. Wuelfing WP, Gross SM, Miles DT, Murray RW. Nanometer Gold Clusters Protected by Surface-Bound Monolayers of Thiolated Poly(ethylene glycol) Polymer Electrolyte. *Journal of the American Chemical Society*. 1998;120(48):12696-12697.
24. Besner S, Kabashin AV, Winnik FM, Meunier M. Synthesis of Size-Tunable Polymer-Protected Gold Nanoparticles by Femtosecond Laser-Based Ablation and Seed Growth. *The Journal of Physical Chemistry C*. 2009;113(22):9526-9531.
25. Robinson I, Alexander C, Lu LT, Tung LD, Fernig DG, Thanh NTK. One-step synthesis of monodisperse water-soluble 'dual-responsive' magnetic nanoparticles. *Chem. Commun*. 2007:4602-4604.
26. Zhang Y, Luo S, Liu S. Fabrication of Hybrid Nanoparticles with Thermoresponsive Coronas via a Self-Assembling Approach. *Macromolecules*. 2005;38(23):9813-9820.
27. Morones JR, Frey W. Environmentally Sensitive Silver Nanoparticles of Controlled Size Synthesized with PNIPAM as a Nucleating and Capping Agent. *Langmuir*. 2007;23(15):8180-8186.

28. Shan J, Tenhu H. Recent advances in polymer protected gold nanoparticles: synthesis, properties and applications. *Chem. Commun.* 2007;4580-4598.
29. Boyer C, Whittaker MR, Luzon M, Davis TP. Design and Synthesis of Dual Thermoresponsive and Antifouling Hybrid Polymer/Gold Nanoparticles. *Macromolecules.* 2009;42(18):6917-6926.
30. Zhou D, Yang L, Yang R, Song W, Peng S, Wang Y. Functionalized gold nanoparticles as additive to form polymer/metal composite matrix for improved DNA sequencing by capillary electrophoresis. *Talanta.* 2009;80(1):195 - 201.
31. Sandström P, Boncheva M, Åkerman B. Nonspecific and Thiol-Specific Binding of DNA to Gold Nanoparticles. *Langmuir.* 2003;19(18):7537-7543.
32. Storhoff JJ, Elghanian R, Mirkin CA, Letsinger RL. Sequence-Dependent Stability of DNA-Modified Gold Nanoparticles. *Langmuir.* 2002;18(17):6666-6670.
33. Ye J, Hou Y, Zhang G, Wu C. Temperature-Induced Aggregation of Poly(N-isopropylacrylamide)-Stabilized CdS Quantum Dots in Water. *Langmuir.* 2008;24(6):2727-2731.
34. Gann JP, Yan M. A Versatile Method for Grafting Polymers on Nanoparticles. *Langmuir.* 2008;24(10):5319-5323.
35. Zubarev ER, Xu J, Sayyad A, Gibson JD. Amphiphilic Gold Nanoparticles with V-Shaped Arms. *Journal of the American Chemical Society.* 2006;128(15):4958-4959.
36. Singh N, Lyon LA. Au Nanoparticle Templated Synthesis of pNIPAm Nanogels. *Chemistry of Materials.* 2007;19(4):719-726.
37. Kang Y, Taton TA. Controlling Shell Thickness in Core-Shell Gold Nanoparticles via Surface-Templated Adsorption of Block Copolymer Surfactants. *Macromolecules.* 2005;38(14):6115-6121.
38. Brewer SH, Glomm WR, Johnson MC, Knag MK, Franzen S. Probing BSA Binding to Citrate-Coated Gold Nanoparticles and Surfaces. *Langmuir.* 2005;21(20):9303-9307.
39. Nordgren N, Rutland MW. Tunable Nanolubrication between Dual-Responsive Polyionic Grafts. *Nano Letters.* 2009;9(8):2984-2990.
40. Turkevich J, Stevenson PC, Hillier J. A study of the nucleation and growth processes in the synthesis of colloidal gold. *Discuss. Faraday Soc.* 1951;11:55-75.
41. Frens G. Controlled Nucleation for the Regulation of the Particle Size in Monodisperse Gold Suspensions. *Nature Physical Science.* 1973;241:20-22.
42. Jones T, Kang I, Wheeler D, Lindquist R, Papallo A, Sabatini D, Golland P, Carpenter A CellProfiler Analyst: data exploration and analysis software for complex image-based screens. *BMC Bioinformatics,* 2008; vol. 9, pp.482
43. Kimling J, Maier M, Turkevich Method for Gold Nanoparticle Synthesis Revisited. *J. Phys Chem B.* 2006; 110, pp. 15700-15707.

44. Israelachvili JN *Intermolecular and Surface Forces*. Elsevier, 2011, Third Edition, ISBN:978-0-12-375182-9
45. D'Souza Mathew, M; Manga, MS; Hunter, TN; Cayre, OJ; Biggs, S Behavior of pH-Sensitive Core Shell Particles at the Air-water Interface. *Langmuir*. 2012; vol. 28, pp.5085-5092.
46. Cayre OJ, Hitchcock J, Manga M, Biggs S pH-responsive colloidosomes and their use for controlling release. *Soft Matter*, 2012; vol. 8, pp.4716-1723.

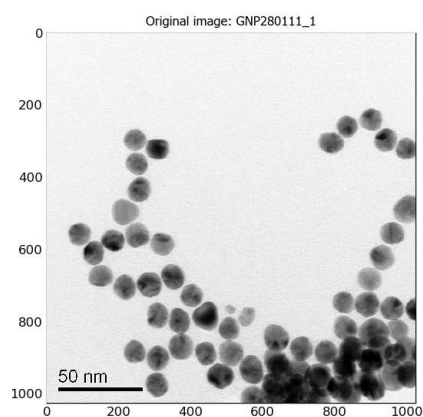
SUPPORTING INFORMATION

Facile synthesis of gold core - polymer shell responsive particles

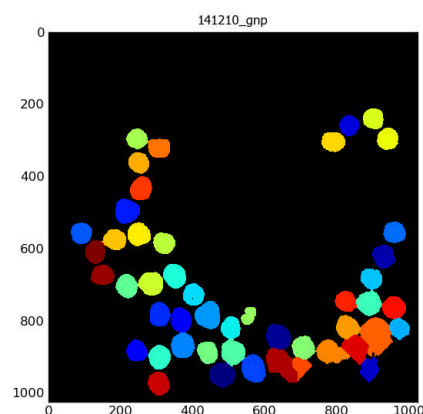
Mark D'Souza Mathew*, Olivier J. Cayre, Timothy N. Hunter and Simon Biggs

*Institute of Particle Science and Engineering
School of Process, Environmental and Materials Engineering
University of Leeds, Leeds, LS2 9JT*

*Email: sms5mdm@leeds.ac.uk

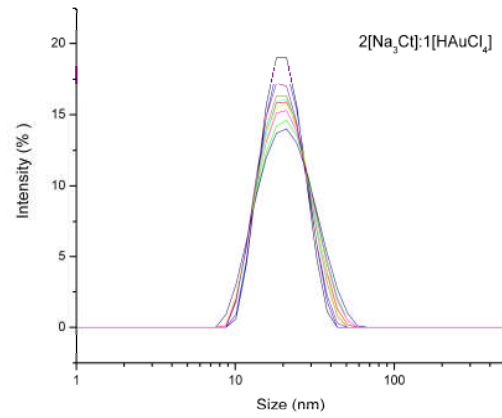


(A)

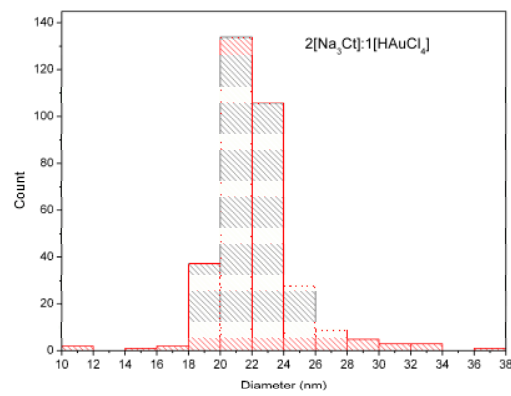


(B)

Figure 1: (A) Transmission Electron Micrograph of citrate stabilized gold nanoparticles. (B) Output from CellProfiler Image analysis software showing identification of individual particles

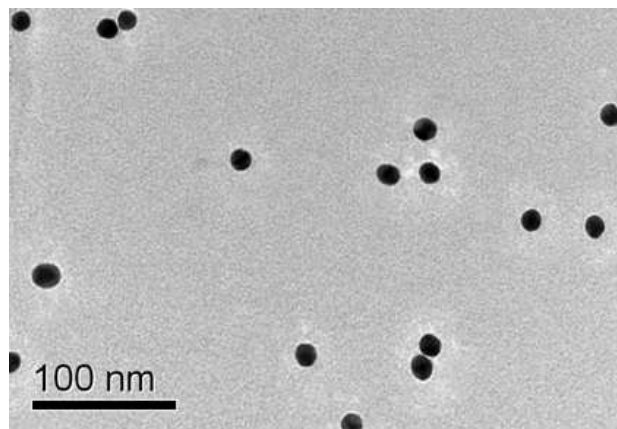


(A)

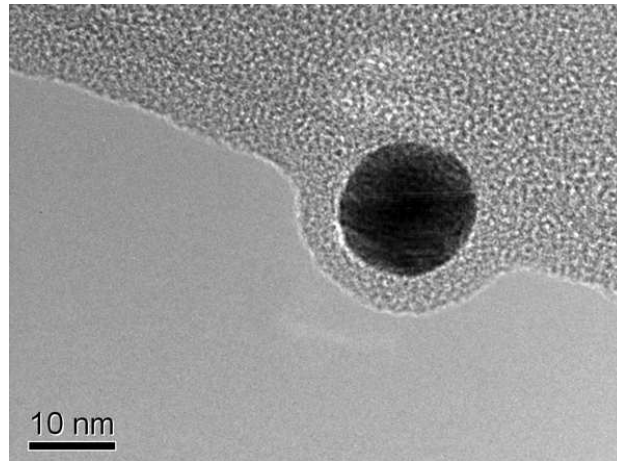


(B)

Figure 2: (A) Multiple intensity profiles of the same citrate stabilized nanoparticles (Figure 1) in an aqueous bulk using Zetasizer for light scattering analysis. (B) Dimensional analysis of particles identified by Cellprofiler with a form factor (indication of roundness) greater than 0.5.



(A)



(B)

Figure 4: (A) TEM images of polymer coated AuNPs dried on holey carbon TEM grids. and (B) Coated particle sitting at the edge of the film with halo possibly attributed to beam damage artefact.

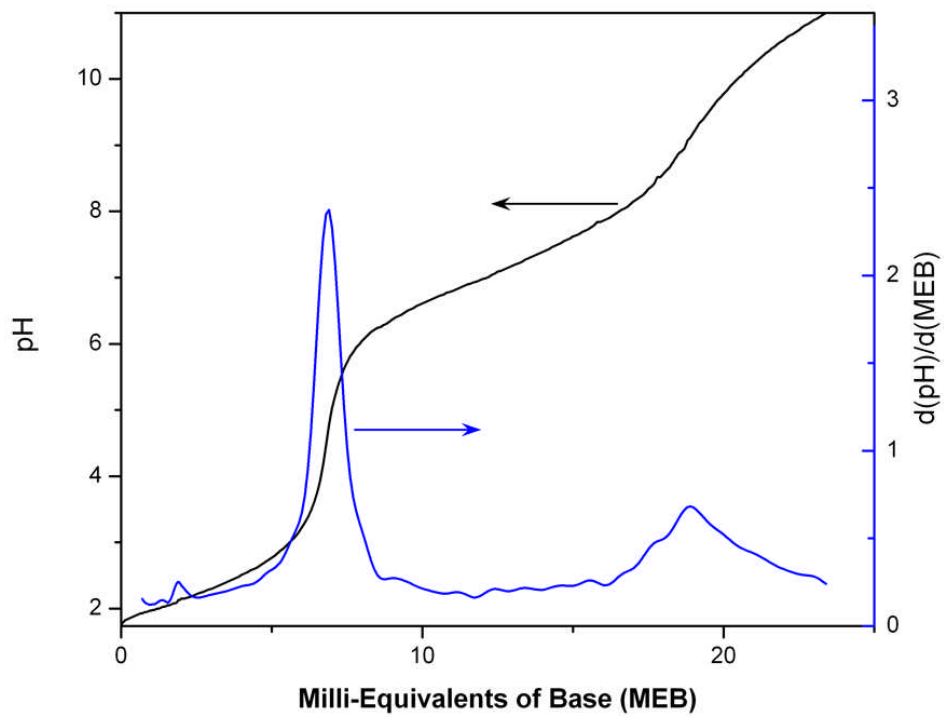


Figure 4: Potentiometric titration of 0.18mM pDMAEMA₁₂₉-SH from pH 1.73 to pH 11.11